Photovoltaic properties of ZnO/CdTe heterojunctions prepared by spray pyrolysis

Julio A. Aranovich, [a] Dolores Golmayo, [b] Alan L. Fahrenbruch, and Richard H. Bube
Department of Materials Science and Engineering, Stanford University, Stanford, California 94305

(Received 21 December 1979; accepted for publication 15 April 1980)

An extended investigation has been made of the electrical and photovoltaic properties of heterojunctions prepared by spray-pyrolysis deposition of thin ZnO films on single-crystal *p*-type CdTe. The principal experimental variables were the substrate temperature and the postdeposition temperature for annealing in H_2. Under actual sunlight the optimum cell showed an open-circuit voltage of 0.54 V, a short-circuit current of 19.5 mA/cm^2, and a solar efficiency (referred to the active area) of 8.8%, the highest value obtained to date for an authentic heterojunction on CdTe. The nature of the forward transport mechanism has been investigated, and a tunneling model in which bulk and interface deep traps control the forward characteristics is shown to provide good correlation with the experimental data.

PACS numbers: 72.40. + w, 73.40.Lq, 81.15.Lm, 73.60.Fw

I. INTRODUCTION

The properties of cadmium telluride make it a prime candidate for the development of thin-film solar cells for terrestrial applications. A growing literature exists on the formation of heterojunctions and buried homojunctions involving CdTe.[1] Solar efficiencies of 8% for an evaporated CdS/CdTe heterojunction[2] and 12% for a junction formed by epitaxial vapor growth[3,4] have been reported. CdS/CdTe [5] and $Zn_x Cd_{1-x}S$/CdTe [6] junctions prepared by spray pyrolysis of the sulfide have been described with efficiencies in the 6–8% range. An all thin-film cell of CdS/CdTe prepared by the screen printing method has been reported to show an efficiency of 8.1%. [7] ITO/CdTe junctions prepared by rf sputtering of ITO onto single-crystal *p*-CdTe have shown efficiencies of 8%. [8] The cells showing the highest efficiencies [3,4,7,8] have been reported to be actually buried homojunction structures induced by the particular preparation method.

ZnO is a material with a band gap large enough (3.3 eV) to be transparent to most of the useful solar spectrum. It can be prepared with a sufficiently low resistivity to prevent series resistance losses in a heterojunction with ZnO as the window layer. The electrical and optical properties of ZnO are the subject of several comprehensive reviews.[9,10] The constituent elements are abundant, the material lends itself to a variety of thin-film deposition techniques, it is nontoxic, and it has a low materials cost. Furthermore, it can be deposited by the simple and inexpensive process of spray pyrolysis; a previously reported investigation[11] showed the conditions under which highly transparent films with resistivity as low as 10^{-3} Ω cm can be produced by suitable control of deposition procedures and by postdeposition annealing in hydrogen. In this paper we take advantage of the previous investigation since it was found that the structural and electrical characteristics of ZnO films deposited on CdTe substrates are similar to those of films deposited on amorphous glass for the range of deposition conditions used here.

In this paper we report the properties of ZnO/CdTe heterojunctions prepared by spray-pyrolysis deposition of ZnO onto single-crystal *p*-type CdTe. By investigating both the effects of postdeposition heat treatment temperature and the effects of substrate temperature during deposition, we have developed an understanding of the current transport processes in these junctions and have been successful in producing a junction with an efficiency of 8.8% (with respect to active area, and 7.6% with respect to total area) under actual sunlight illumination. This is the highest efficiency to be reported for an authentic heterojunction on CdTe.

An "ideal" heterojunction band diagram constructed following the Anderson[12] model for the ZnO/CdTe system is shown in Fig. 1. In this model it is assumed that no interfacial charge or dipoles are present. The junction barrier, totally located on the *p*-type CdTe side since the ZnO is degenerate, is too thick to allow for sizable tunneling currents. The configuration shown implies that the forward current mechanism is diffusion of minority carriers (electrons) into the quasineutral *p*-type side of the junction and/or recombination of carriers if a high density of recombination centers

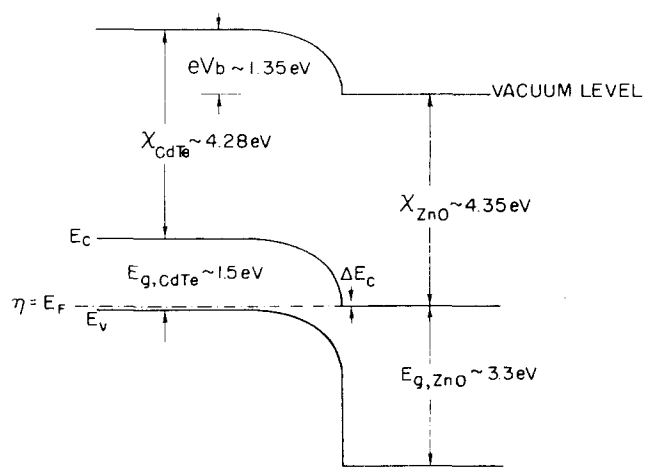

FIG. 1. "Ideal" ZnO/CdTe heterojunction band diagram constructed following Anderson's model; for CdTe doping of 10^{17} cm^{-3}, the depletion layer width is about 0.1 μm.

[a] Present address: Hewlett-Packard, Cupertino, California.
[b] Permanent address: I.F.M., Serrano 144, Madrid, Spain.

 0021-8979/80/084260-09$01.10

is assumed to be present in the depletion region or at the metallurgical interface. In either case, the diode parameter $\alpha = (q/AkT)$, where $J = J_0[\exp(\alpha V) - 1]$, with $A = 1$ for the diffusion case and $A = 1$–2 for recombination currents. We do not, in fact, find this kind of behavior with our ZnO/CdTe junctions: the value of α is only slightly temperature dependent, and the measured values of J_0 are much larger than those calculated from diffusion or recombination theory. This is, in fact, fairly standard behavior for many different kinds of heterojunctions, for which bulk and interfacial defects are more the rule than the exception. Deep acceptor levels in the CdTe and/or negative interfacial charge result in a considerable narrowing of the junction barrier, increasing the tunneling probability for holes so that forward-bias tunneling currents become dominant. The results presented in Secs. II–VII lead us to this conclusion.

II. MATERIALS

The P-doped CdTe crystal boule used in this research was grown[13] by the Bridgman method with excess Te added to favor p-type conduction and to prevent ampoule explosion. The crystal was subsequently zone refined. Four-point resistivity measurements on the boule indicated that the material had an average resistivity of 1 Ω cm, corresponding to an estimated hole density of about 10^{17} cm^{-3}. Wafers were cut starting from the most uniform (beginning) end of the boule, and were labeled in alphabetical order, (a), (b)···, as they approached the region where impurities and excess P and Te had been zoned out. The substrates, about 5×3 mm^2, were polished and chemically etched until mirrorlike surfaces with no defects were obtained.

ZnO films were deposited by spray pyrolysis to a thickness of about 0.5 μm, according to the description previously published,[11] either from $ZnCl_2$ solution (ZOT cells) or from Zn acetate solution (ZOAT cells). A total of about 40 cells were prepared and given at least a partial analysis; this paper draws on specific data from a few of these that were most completely analyzed.

III. EFFECTS OF HEAT TREATMENT IN HYDROGEN

The dark and light J-V characteristics in the as-deposited ZnO/CdTe junctions were quite poor, but in all cases heat treatment in hydrogen produced a marked improvement in the overall cell behavior.

A typical development of the dark and light J-V characteristics with increasing heat treatment temperature in hydrogen is illustrated in Figs. 2 and 3 for an exploratory cell, ZOTO-10. In the as-deposited condition, forward and reverse bias currents are large at low bias, the forward J-V dependence does not follow $J = J_0[\exp(\alpha V) - 1]$, the saturation of current with increasing forward bias cannot be satisfactorily described as a series-resistance effect, the reverse breakdown voltage is low, and the zero-bias capacitance is unexpectedly large. Illumination of the as-deposited junction shows appreciable short-circuit current magnitudes (10 mA/cm^2 for as-deposited ZOTO-10), in spite of cross-over of the dark and light J-V curves, a large displacement of the ln J_{sc}-vs-V_{oc} curve from the dark ln J-vs-V curve, and a slow

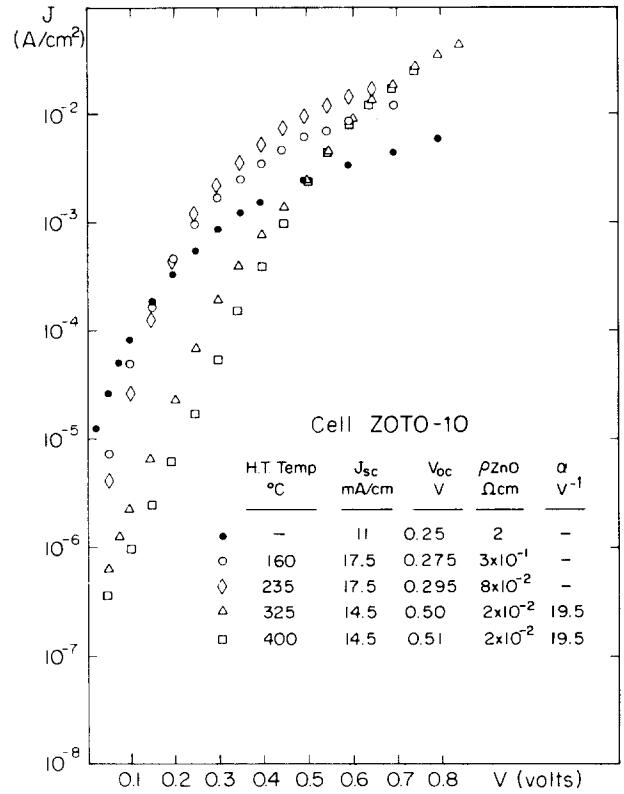

FIG. 2. Forward dark J-V characteristics of cell ZOTO-10 as a function of heat-treatment temperature in hydrogen.

increase in the zero-bias junction capacitance with time. However, open-circuit voltage values were typically only 0.2 V, and fill factors were of the order of 0.35.

Heat treatment at up to 235 °C showed modest improvement in the diode characteristics but a large increase in short-circuit current to 17.5 mA/cm^2, indicating that collection of photogenerated carriers was highly efficient in spite of the poor junction behavior in the dark. For heat treatment at 325 °C, however, a much larger change in the characteristics of the cell was observed. The dark J-V characteristics became exponential with $\alpha = 20.5$ V^{-1} at 300 °K, the reverse breakdown voltage increased significantly, and the open-circuit voltage increased to 0.50 V. Further increase of the heat treatment to 400 °C produced a noticeable but small improvement of the cell behavior, mainly through a reduction in the value of J_0. The reduction of J_{sc} shown for cell ZOTO-10 with heat treatment is not typical of general results, which indicate that a single heat treatment up to 400 °C need not cause a loss of J_{sc}.

Heat treatment at a temperature of 430 °C for 5 min was found to be the maximum that could be used without degrading the cell; longer times and higher temperatures resulted in degradation of film quality, probably due to precipitation of a Zn-rich second phase in the ZnO. The effects of heat treatment were investigated in several other cells grown under a variety of different conditions; similar results were observed for all such cells. Consequently, this was the heat treatment subsequently used for all other cells.

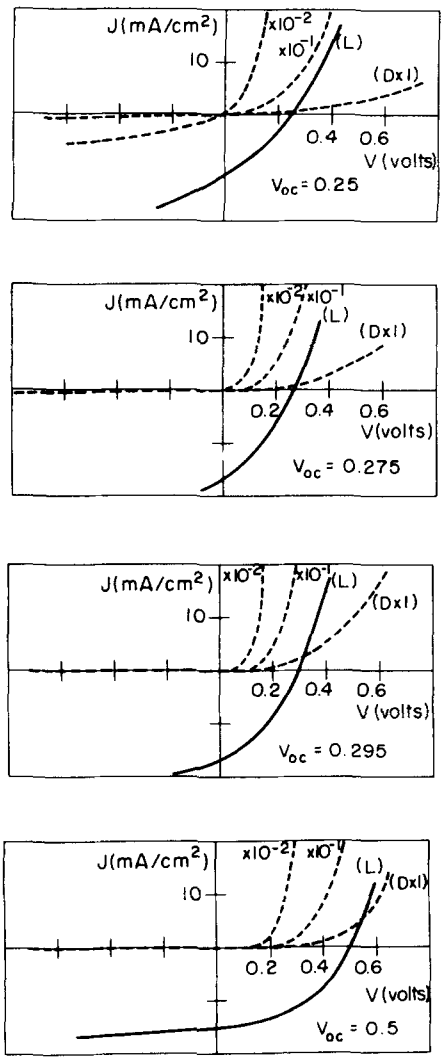

FIG. 3. Dark and light J-V characteristics of cell ZOTO-10 for different heat-treatment conditions. The dark data (dashed curves) are shown for several different current scale sensitivities.

IV. EFFECT OF SUBSTRATE TEMPERATURE

A series of cells was prepared at different substrate temperatures for the spray-pyrolysis deposition, with the results summarized in Table I. After deposition, cells were heat treated at 430 °C in hydrogen for 5 min, stored in the dark until stable dark characteristics were obtained, and then exposed to simulated sunlight just prior to measurement of the light characteristics. The results show that optimum behavior was obtained for a substrate temperature of 460 °C.

Dark and light characteristics of representative cells prepared at substrate temperatures of 470 °C or less are shown in Figs. 4 and 5. As the substrate temperature is increased from 430 to 460 °C, the dark J-V characteristics improve considerably and shift toward higher bias voltages, remaining almost parallel to one another and exhibiting a strong reduction in J_0 with increasing preparation substrate temperature T_s. The reverse current characteristics show a similar improvement. The zero-bias capacitance values were larger than expected from the CdTe carrier density.

Under simulated solar illumination, large values of short-circuit current were observed: typically of the order of 20 mA/cm^2 for illumination of 87 mW/cm^2 for T_s less than 470 °C. The spectral response (at J_{sc}) of the quantum efficiency shown in Fig. 6 for three of the cells was essentially panchromatic between the band gaps of ZnO and CdTe, as would be expected for a heterojunction cell. The solar conversion efficiency increased markedly with increasing T_s up to 460 °C, primarily because of an increase in V_{oc} and a fill factor which can be correlated with the decrease in J_0. All cells showed cross-over of the dark and light characteristics and a displacement of the ln J_{sc}-vs-V_{oc} curve from the dark ln J-vs-V curve, indicating a strong dependence of the forward current on illumination. Illumination decreased the reverse breakdown voltage and increased the zero-bias capacitance.

TABLE I. Junction and photovoltaic properties of selected ZnO/CdTe cells.

Cell No.[a]	T_s(°C)	V_{oc} (V)	J_{sc} (mA/cm^2) Total area	J_{sc} (mA/cm^2) Active area	J_0 (A/cm^2)	α (V^{-1})	V_B (V)	Spectral response
ZOT[a] −2	430	0.31	16.1	20.9	8.0×10^{-6}	23.9	...	Panchromatic
ZOAT[a] −2	415	0.15	11.4	14.0	4.0×10^{-5}	27.1	...	Panchromatic
ZOAT[a] −3	430	0.31	18.1	19.3	2.2×10^{-6}	27.1	3.7	Panchromatic
ZOT[a] −3	445	0.40	18.1	19.3	4.7×10^{-7}	27.1	5.1	Panchromatic
ZOT[a] −4	460	0.53	18.2	21.1	3.7×10^{-9}	27.1	7.0	Panchromatic
ZOT[b] −17	470	0.45	16.9	19.6	2.0×10^{-7}	23.3	7.1	Panchromatic
ZOT[c] −26	470	0.40	16.3	...	...	...	...	Panchromatic
+ Air HT		0.28	17.7	...	6.9×10^{-6}	21.8	...	...
+ Air HT		0.28	4.6	...	1.0×10^{-6}	21.8	8.7	Decreasing for higher photon energies
+ H_2 HT		0.50	10.4	...	3.5×10^{-8}	21.8	9.4	Decreasing for higher photon energies
ZOT[c] −24	490	0.25	15.6	...	...	...	...	...
+ Air HT		0.29	11.1	...	5.0×10^{-6}	21.8	...	Decreasing for higher photon energies
+ Air HT		0.24	2.1	...	1.6×10^{-7}	21.8	11.0	Decreasing for higher photon energies

[a]Alphabetical superscript on Cell No. indicates the wafer from which the substrate was cut, beginning from the end of the boule at which growth was initiated.

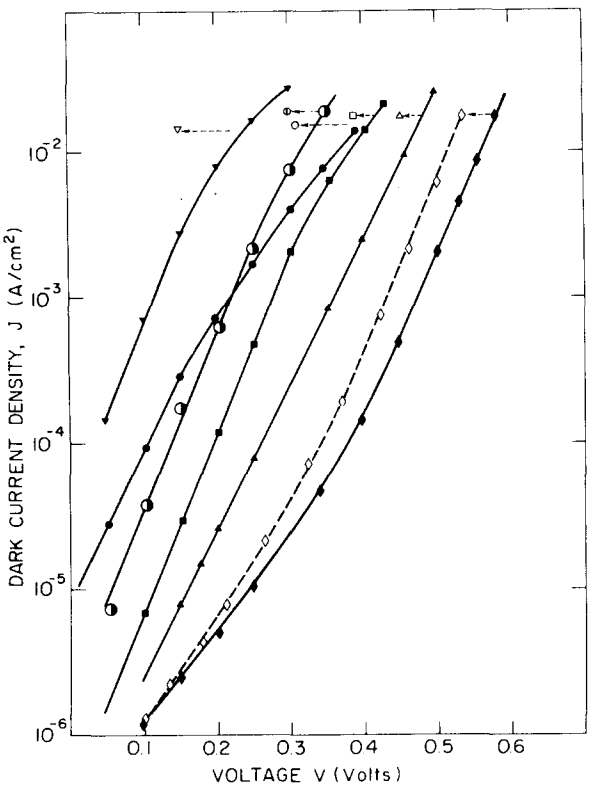

FIG. 4. Dark J-V characteristics for selected heat-treated cells prepared at different substrate temperatures and J_{sc}-V_{oc} data under solar simulation. The first symbol in each case represents the dark data, and the second symbol the light data: (▼, ▽) ZOAT[a] −2, T = 415 °C; (◑, Φ) ZOAT[a] −3, T_s = 430 °C; (●, ○) ZOT[a] −2, T_s = 430 °C; (■, □) ZOT[a] −3, T_s = 445 °C; (◆, ◇) ZOT[a] −2, T_s = 460 °C; (▲, △) ZOT[b] −17 T_s = 470 °C.

For T_s greater than 460 °C, a definite degradation in the current characteristics was observed. Figure 4 shows that a substrate temperature of 470 °C results in an increase in J_0, which then manifests itself as a decrease in V_{oc}, fill factor, and solar efficiency. The short-circuit current also decreased and the spectral dependence of the quantum efficiency showed a decrease with increasing photon energy, a departure from typical heterojunction behavior. The spectral dependence for a cell made with T_s = 490 °C is shown for comparison in Fig. 7, showing this effect.

Consideration of possible causes of this degradation effect for high T_s suggests that a heat treatment in air might ameliorate the situation: (a) a higher density of interfacial defects associated with the higher T_s might be annealed away with further heat treatment, but a further heat treament in hydrogen would cause zinc precipitation; (b) precipitation of zinc might have been caused by the higher T_s, and annealing in an oxidizing atmosphere might reduce this effect. In any event, heat treatment in air did markedly improve the dark J-V characteristics of cells prepared with T_s = 470 and 490 °C, as shown in Fig. 8. However, the quantum efficiency and short-circuit current decreased monotonically with the length of this heat treatment in air, as shown in Table I.

V. ANALYSIS OF AN EXPERIMENTAL CELL

The best behavior obtained in this present series of experiments was obtained with cell ZOT-4 prepared at 460 °C on an (a) substrate. This cell had a total area of 0.15 cm^2 and an active area of 0.13 cm^2. A solar efficiency of 9.2% (based on active area) was obtained for simulated solar illumination (Fig. 5). This cell was also measured under actual sunlight conditions, with the results shown in Fig. 9; the measured solar efficiency of 8.8% (based on the active area) is the largest to be reported for an authentic heterojunction on CdTe.

The temperature dependence of the dark J-V characteristics for this cell are shown in Fig. 10. A second exponential region at low bias voltages can be disregarded for present purposes since it plays no role in the practical photovoltaic behavior of the cell. The diode parameter α does not equal (q/AkT) since it varies much more slowly with temperature, suggesting that the forward controlling mechanism is tunneling across the CdTe junction barrier. The dark J-V parameters for this cell are summarized in Table II.

The data of Fig. 4 for this cell indicate a relatively large displacement of the ln J_{sc}-vs-V_{oc} curve from the dark ln J-

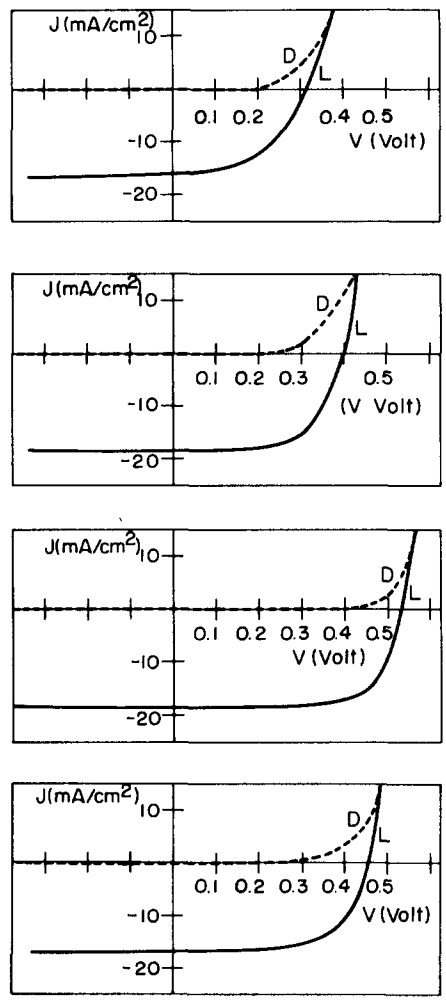

FIG. 5. Dark and light J-V characteristics of heat treated cells prepared at different substrate temperatures. From the top: ZOT[a] −2, T_s = 430 °C; ZOT[a] −3, T_s = 445 °C; ZOT[a] −4, T_s = 460 °C; ZOT[b] −17, T_s = 470 °C.

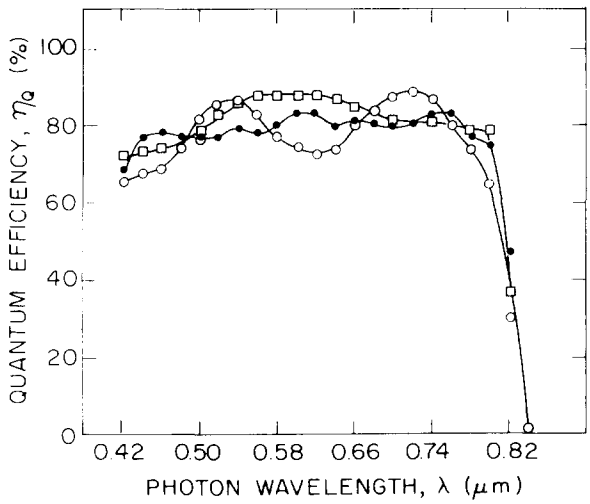

FIG. 6. Spectral dependence of the quantum efficiency of heat-treated cells prepared at different substrate temperatures. (○) ZOT[(a)]-2, T_s = 415 °C; (●) ZOT[(a)]-4, T_s = 460 °C; (□) ZOT[(a)]-17, T_s = 470 °C. Structure in the curves is due to interference effects.

vs-V curve, indicating light dependence of the forward current mechanism. A cross-over of the light and dark characteristics was observed in this cell.

The magnitude of the short-circuit current could be increased by applying a reverse bias, as indicated in Fig. 11. This effect suggests that the collection efficiency depends on the local electric field at the interface and is an indication of the control of interface recombination by this electric field. This effect was observed in all cells.

The temperature dependence of the open-circuit voltage is shown in Fig. 12. The high-temperature values can be fit by a straight line extrapolating to V_{oc} (0 °K) = 1.15 V.

The reverse breakdown voltage decreases monotonically as the temperature is decreased, indicating that avalanche multiplication controls the reverse junction breakdown. The change is relatively small, decreasing from 7.5 V at 350 °K to 5.8 V at 215 °K.

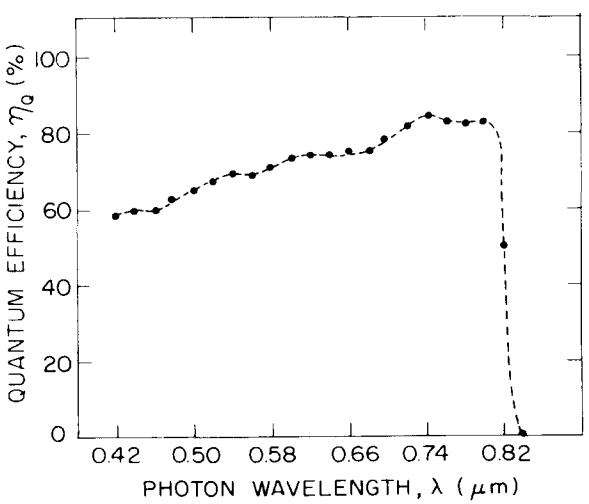

FIG. 7. Spectral dependence of the quantum efficiency for a heat-treated cell prepared at high substrate temperature: ZOT[(b)]-11, T_s = 490 °C.

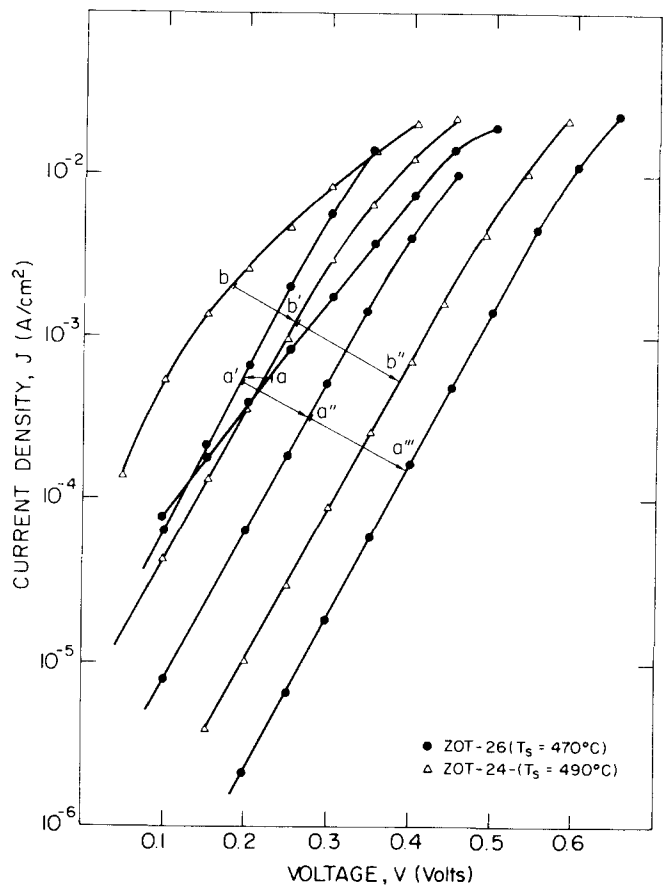

FIG. 8. Dark J-V characteristics of two heat-treated cells prepared at high substrate temperatures: (●) ZOT[(c)]-26, T_s = 470 °C; (Δ) ZOT[(c)]-24, T_s = 490 °C. Curves (a) and (b) are the characteristics after the standard hydrogen treatment; (a′) and (b′) after a second heat treatment, in air at 460 °C; (a″) and (b″) after a third heat treatment, in air; and (a‴) after a final heat treatment in hydrogen at 430 °C.

VI. DISCUSSION

A. General aspects

The general aspects of a model describing the behavior of these ZnO/CdTe junctions are developed from the following inputs:

(1) The small temperature dependence of the diode parameter α as well as the magnitude of J_0 suggests that the dark forward current is controlled by tunneling of holes through the CdTe junction barrier.

(2) The magnitudes of the diode parameter and J_0 indicate that tunneling must take place through a much narrower effective depletion region than that predicted from the nominal doping of the CdTe.

(3) This hypothesis of a narrow depletion region is supported by all of our other measurements: high junction capacitance, small reverse breakdown voltages, and large reverse currents.

(4) Departure from the optimum cell-fabrication conditions causes still narrower depletion regions, as indicated by the increase in tunneling currents, the increase in reverse currents, the decrease in the reverse breakdown voltage, and the increase in junction capacitance.

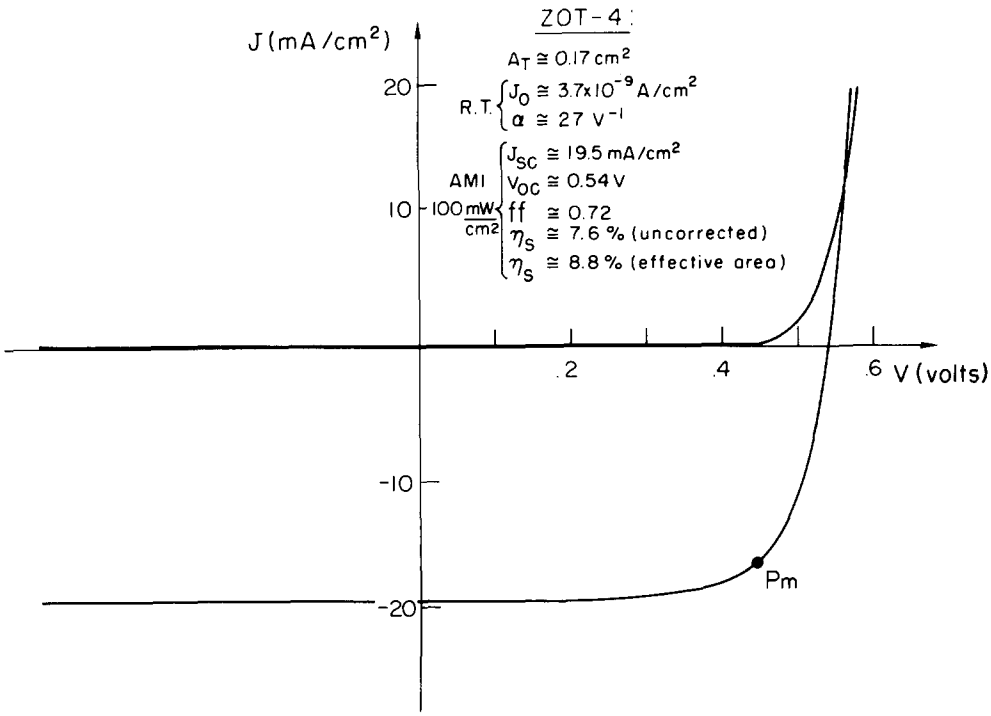

FIG. 9. Dark and light J-V characteristics of cell ZOT(-4) under actual solar illumination of 100 mW/cm^2 with a spectral distribution of approximately AM1.

(5) The fact that illumination causes an increase in the junction capacitance, an increase in forward tunneling currents, and a decrease in reverse breakdown voltage suggests that the principal effect of light is to further decrease the junction barrier width.

(6) The observation of slow transient effects in the dark and light characteristics, slow changes of the junction capacitance with illumination, and slow recovery of the initial electrical characteristics after exposure to light suggest that the narrowing of the depletion layer must be at least partially associated with centers with a population governed by slow kinetics. These phenomena are more prominent the greater the departure from optimum preparation conditions.

(7) The saturation of forward-bias currents with increasing bias voltage occurs at lower bias voltages with increasing departure from optimum preparation conditions.

(8) Cells produced on CdTe substrates cut from the same wafer show exactly the same diode parameter with heat treatment even though the value of J_0 varies by orders of magnitude. Cells produced with different wafers show small but definite differences in the value of the diode parameter, which varies directly with position of the wafer in the crystal boule.

B. Dark current transport model

The temperature dependence of the diode parameter α observed on cell ZOT-4 is qualitatively well described by the theoretical model of Tansley[14] using a numerical calculation to accurately describe tunnel currents in one-sided junctions. In order to obtain quantitative information, the approximate analytical model developed by Padovani and Stratton[15] for tunneling currents in Schottky barriers is used here. The forward tunneling current in a one-sided ZnO/CdTe heterojunctions is expressed as

$$J = J_0[\exp(\alpha V) - 1] \tag{1}$$

$$= J_{00}\exp(-\alpha V_b)[\exp(\alpha V) - 1], \tag{2}$$

with

$$\alpha = q(E_0)^{-1}, \tag{3}$$

$$E_0 = E_{00}\coth(E_{00}/kT), \tag{4}$$

$$E_{00} = (\tfrac{1}{2}q\hbar)(N_A/\epsilon m^*)^{1/2} \tag{5}$$

$$J_{00} \simeq \frac{A^* E_{00}^{1/2}(qV_b + \eta - qV)^{1/2}}{kT\cosh(E_{00}/kT)}\exp\left[\eta\left(\frac{1}{kT} - \frac{\alpha}{q}\right)\right]. \tag{6}$$

Here V_b the CdTe junction barrier height at equilibrium, N_A is the effective dopant density in the depletion region, ϵ and m^* are the dielectric constant and the effective mass for holes in CdTe, respectively, $A^* \propto T^2$ is an effective Richardson constant, and η is the separation between the hole quasi-Fermi level and the valence band.

The measured values of the diode parameter α for cell ZOT-4 as a function of temperature are plotted in Fig. 13, where they are compared with calculated values using Eq. (3) for different effective doping densities. A good fit is obtained for an effective doping density of 2.5×10^{18} cm^{-3}. This is in good agreement with other electrical estimates of the effective doping density: the zero-bias capacitance of the cell gives a value of 1.8×10^{18} cm^{-3}, and the 300 °K reverse breakdown voltage indicates a doping of the order of 10^{18} cm^{-3}.

Furthermore, if the model applies, a plot of $\ln[J_0\times\cosh(E_{00}/kT)]/T$ versus α should give a straight line with slope equal to the CdTe junction barrier height.[15] Such a plot is given in Fig. 14 for the measured J_0 and α values of cell ZOT-4. The data can be well fit by a straight line with a slope of 1.35 V. The good agreement between this value and the calculated CdTe junction barrier height in Fig. 1 is encour-

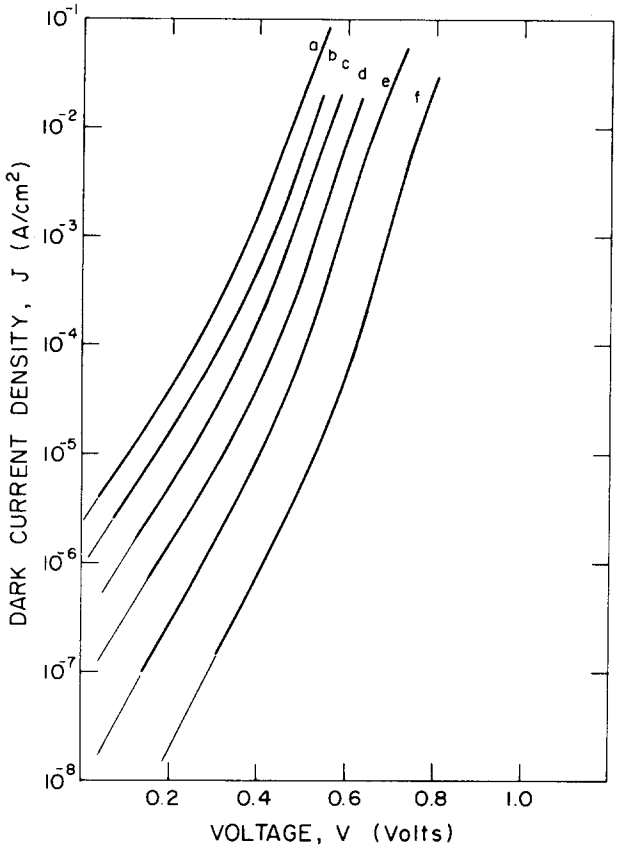

FIG. 10. Temperature dependence of the dark J-V characteristics for cell ZOT [a]-4. See Table II for tabulated data. (a) 339 °K, (b) 319 °K, (c) 297 °K, (d) 273 °K, (e) 241 °K, and (f) 176 °K.

aging but must be taken with some caution in view of the limited assumptions underlying the construction of Fig. 1 and the approximate values of V_b obtained by applying the simple tunneling model.

The fact that the extrapolated value of the open-circuit voltage to 0 °K is 1.15 V is consistent with this estimation of the barrier height if the light dependence of the forward current is considered. Only in ideal situations does V_{oc} (0 °K) = V_b. If V_b = 1.35 V is assumed and Eq. (2) used, modifying J_{00} to take into account the departure of the ln J_{sc}-vs-V_{oc} curve from the ln J-vs-V curve, and assuming that both this departure and the short-circuit current are temperature independent, an expected value of V_{oc} can be calculated as a function of temperature using the temperature dependence of the diode parameter. The result of such a calculation is shown in Fig. 12, where good agreement is found for the high-temperature range.

TABLE II. Temperature dependence of the dark J-V characteristics of cell ZOT [a]-4 (see Fig. 10).

Figure 10 curve	T (°K)	J_{01} (A/cm²)	α_1 (V⁻¹)	J_{02} (A/cm²)	α_2 (V⁻¹)
a	339	7.1×10^{-8}	25	2.2×10^{-6}	13.6
b	319	1.6×10^{-8}	26	9.0×10^{-7}	14.4
c	297	3.7×10^{-9}	27.1	2.8×10^{-7}	14.8
d	273	2.8×10^{-10}	28.8	7.4×10^{-8}	15.2
e	241	1.6×10^{-11}	30.5	9.0×10^{-9}	17.2
f	176	9.0×10^{-14}	33.5	8.0×10^{-10}	18.8

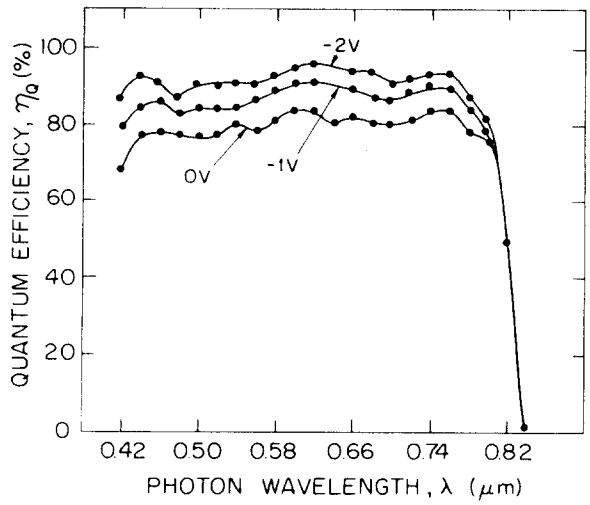

FIG. 11. Spectral dependence of the quantum efficiency for cell ZOT [a]-4 with and without applied reverse bias.

Since all the electrical measurements indicate that the charge density in the depletion region is of the order of 10^{18} cm^{-3}, an order of magnitude greater than the nominal doping of 10^{17} cm^{-3} of the CdTe crystal, two possibilities suggest themselves: (a) the actual doping is larger than expected by an order of magnitude; or (b) deep acceptorlike centers become ionized upon junction formation. The second of these possibilities seems the more likely. Additional evidence for this conclusion follows.

The data from Figs. 4 and 8 show that the dark ln J-V characteristics of cells prepared on CdTe substrates from the same wafer are parallel. Equations (3)–(5) show that the slope of the ln J-V curves, i.e., the diode parameter α, depends only on the effective doping N_A. As a first approximation, the CdTe crystal boule has axial symmetry; owing to zone refining there is an increasing density of impurity accumulation away from the purer end of the boule, with primarily excess Te and P being zoned out. Resistivity measurements made before the boule was cut confirm the

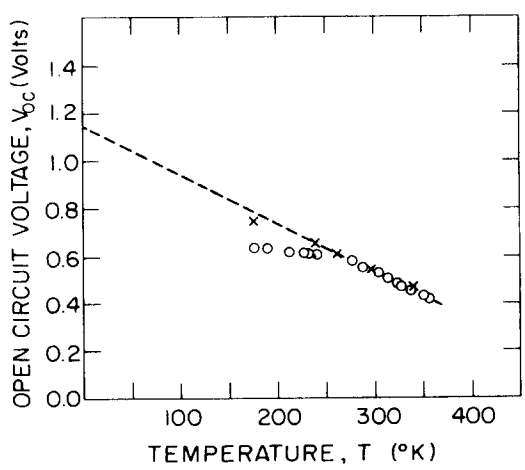

FIG. 12. Temperature dependence of the open-circuit voltage of cell ZOT [a]-4 under simulated sunlight. (○) measured values; (×) values calculated from the dark characteristics of the cell as described in the text.

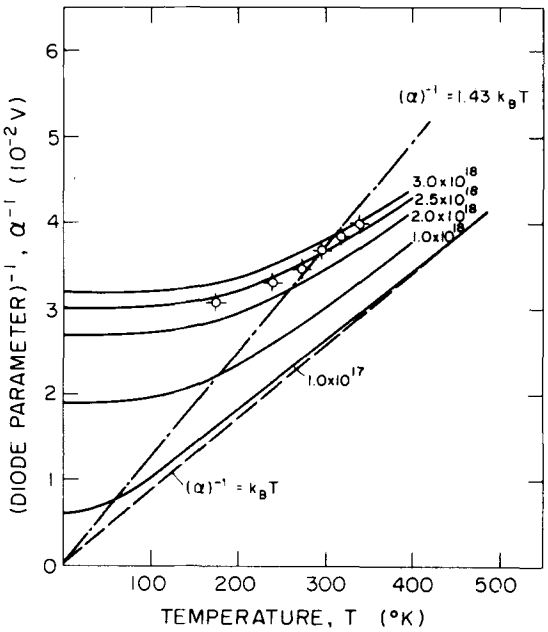

FIG. 13. Temperature dependence of the reciprocal diode parameter for various doping densities. The expected theoretical behaviors are as follows: (———) tunneling model; (- - - -) diffusion model, (— — — — —) recombination model with $A = 1.43$. $k_B = k/q$.

expectation that the effective doping increases with the wafer sequence (a), (b), (c), etc. Table I shows that the diode parameter decreases as expected for successive wafers in this sequence. To further confirm this hypothesis, an In/CdTe Schottky barrier was prepared by vacuum evaporation of In using a CdTe substrate from wafer (d), still closer to the impure end of the boule; the J-V characteristics of this junction were similar to those for ZnO/CdTe junctions with an even smaller diode parameter and larger J_0 value, as expected.

Since the diode parameter α is the same for cells prepared from the same wafer, the only difference between their ln J-V characteristics is the factor J_0. Equation (2) shows that large changes in J_0 must be attributed to a change in the junction barrier height V_b. Negatively charged interfacial states produce an increase in the potential at the interface, consequently reducing V_b (the increase in the barrier height in the n-type side has a negligible effect since the ZnO is degenerate). It appears reasonable, therefore, to propose that the approximately parallel displacement of the ln J-V characteristics is a consequence of an increasing density of negatively charged interfacial states as we depart from optimum conditions. This density of interfacial states depends both on the preparation conditions and the specific window material.

The junction barrier height for different cells showing parallel ln J-V characteristics in Fig. 4 can be estimated from the measured J_0 values, using the calculated V_b for cell ZOT-4 as a reference. The junction barrier heights determined in this way for different cells are summarized in Table III.

We also propose that deep acceptorlike centers at the interface and in the bulk of the CdTe play a key role in tunneling transport phenomena and in current saturation effects observed in the ln J-V curves. Large tunneling currents are observed when the traps are ionized, since they produce an effective narrowing of the junction. As forward bias is applied, the Fermi level approaches the trap level at the interface, and the effect of traps becomes less important as fewer traps are ionized. When the Fermi level crosses the energy levels of the traps at the interface, all the traps become nonionized and the shape of the potential barrier is controlled entirely by the shallow acceptors as if the deep traps were not present. Consequently, tunneling becomes less efficient and saturation is observed in the ln J-V plots. We can make a simplified test of this approach in the following way. Suppose that the position of the trap levels is the same for each of the cells listed in Table III. As the junction barrier height is decreased, the position of the trap level at the interface is lower and a smaller forward bias is needed to bring the Fermi level close to the trap position. Current satu-

TABLE III. Calculated CdTe junction parameters.

Cell No.	V_b (V)[a]	$V_b - V_{sat}$ (V)[b]
ZOT[(a)] −3	1.17	0.87
ZOAT[(a)] −3	1.12	0.87
ZOAT[(a)] −2	1.01	0.85

[a]Junction barrier height with reference to ZOT[(a)] −4, assuming $V_b = 1.35$ V for ZOT[(a)] −4.

[b]Difference between the forward-bias voltage for the onset of current saturation and the value of V_b from column two.

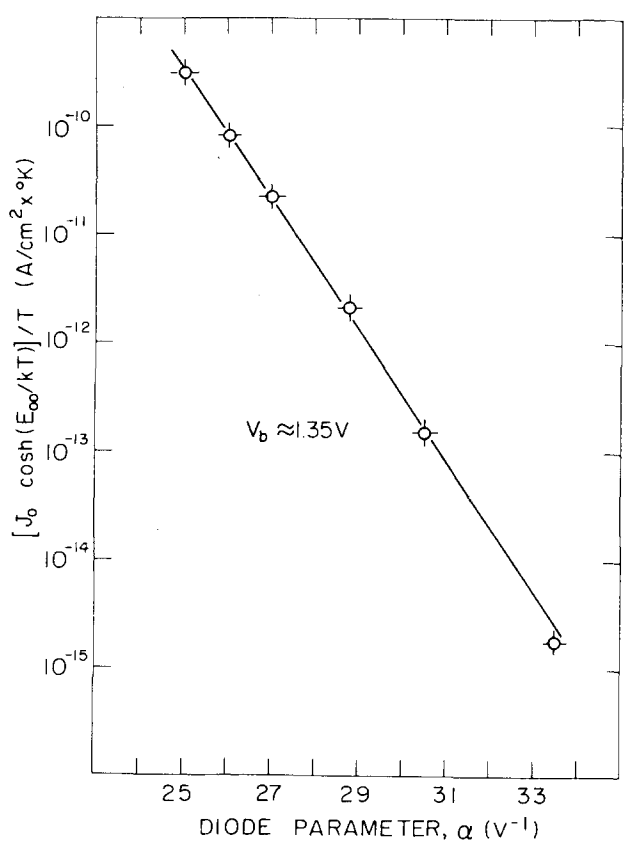

FIG. 14. Dependence of $J_0[\cosh(E_{00}/kT)]/T$ on the diode parameter.

ration, therefore, takes place at a lower forward bias for lower junction barrier heights, as observed. If we take as a first approximation the difference between the barrier height and the bias for the onset of saturation as an indication of the location of the trap level, we can see if this value is approximately the same for the cells of Table III. The values listed in Table III indicate that this is indeed the case, the difference $(V_b - V_{sat}) \simeq 0.86$ V for all three cells.

The improvement in junction characteristics observed with increasing substrate temperature up to 460 °C may have several possible explanations. The density of the interface states may depend on the orientation of the film; preferential orientation increases as a characteristic temperature is reached, this temperature being 440 °C for films deposited on glass. *In situ* thermal annealing during growth may reduce the density of interface states as postdeposition annealing does, and therefore improve junction characteristics with increasing deposition temperature until a crucial temperature is reached at which other degradation mechanisms come into play. Finally, there is the possibility that a very thin insulating interfacial layer builds up with increasing substrate temperature; if this layer is transparent to electrons, it does not cause a decrease in J_{sc}, but a reduction in J_0 can result from either partial opacity of the layer to holes or an increase in the junction barrier height due to fixed stored charge within the layer.

In the presence of illumination, photogenerated electrons drift in the junction field and are trapped by the interfacial states, producing a decrease in the junction barrier height and an increase in the forward tunneling current; an increase in junction capacitance and a reduced reverse breakdown voltage are also observed owing to corresponding narrowing of the junction width. The interface states are characterized by a slow kinetics in the dark and in the light, reminiscent of the kind of slow surface traps characteristic of ZnO. Because of the slow kinetics, transient and hystersis effects are observed. As the density of surface states is reduced, this effect becomes less important.

VII. SUMMARY

ZnO/CdTe junction solar cells have been prepared by the spray-pyrolysis deposition of ZnO films onto single-crystal p-type CdTe. By controlling the CdTe substrate temperature during deposition and the postdeposition heat treatment in hydrogen, cells have been produced with solar efficiency in actual sunlight as high as 8.8% referred to the active area of the cell. In spite of an extremely large lattice mismatch between ZnO and CdTe (28%), quantum efficiencies of 80% are readily achieved without applied bias, and greater than 90% with applied reverse bias. The spectral response of the quantum efficiency is that expected for a heterojunction.

It is proposed that a large density of negatively charged interface states are produced upon junction formation, which produce a large decrease in the junction barrier height. As the cells are annealed, the density of these interfacial states is reduced, the junction barrier height is increased, and the ln J-V characteristics are displaced toward higher bias voltages because of a decrease in J_0. Deep acceptorlike levels lying 0.86 eV above the valence band in the bulk of the CdTe shrink the depletion-layer width and give rise to large tunneling currents. The forward current saturates in a ln J-V plot when sufficient forward bias is applied to raise the Fermi level above the level associated with these deep levels.

ACKNOWLEDGMENTS

This research was supported by the Materials Science Program, Division of Basic Energy Sciences, Department of Energy.

[1] R. H. Bube, F. Buch, A. L. Fahrenbruch, Y. Y. Ma, and K. W. Mitchell, IEEE Trans. Electron Dev. **ED-24**, 487 (1977).
[2] K. Mitchell, A. L. Fahrenbruch, and R. H. Bube, J. Appl. Phys. **48**, 4365 (1977).
[3] K. Yamaguchi, H. Matsumoto, N. Nakayama, and S. Ikegami, Jpn. J. Appl. Phys. **15**, 1575 (1976).
[4] K. Yamaguchi, N. Nakayama, H. Matsumoto, and S. Ikegami, Jpn. J. Appl. Phys. **16**, 203 (1977).
[5] Y. Y. Ma, A. L. Fahrenbruch, and R. H. Bube, Appl. Phys. Lett. **30**, 423 (1977).
[6] S. Y. Lin, A. L. Fahrenbruch, and R. H. Bube, J. Appl. Phys. **49**, 1294 (1978).
[7] N. Nakayama, H. Matsumoto, K. Yamaguchi, S. Ikegami, and Y. Hioki, Jpn. J. Appl. Phys. **15**, 2281 (1976).
[8] F. G. Courreges, A. L. Fahrenbruch, and R. H. Bube, J. Appl. Phys. **51**, 2175 (1980).
[9] H. E. Brown, *Zinc Oxide Rediscovered* (The New Jersey Zinc. Co., New York, 1957).
[10] G. Heiland, E. Mollwo, and F. Stöckmann, Solid State Phys. **8**, 193 (1959).
[11] J. Aranovich, A. Ortiz, and R. H. Bube, J. Vac. Sci. Technol. **16**, 994 (1979).
[12] R. L. Anderson, IBM Thomas J. Res. Dev. **4**, 283 (1960).
[13] CdTe crystals were grown by R. Raymakers of the Crystal Growth Laboratory, Center for Materials Research, Stanford University.
[14] T. L. Tansley, in *Semiconductors and Semimetals*, edited by R. K. Willardson and A. C. Beer (Academic, New York, 1971), Vol. 7A, Chap. 6.
[15] F. A. Padovani, Ref. 14, Chap. 2.